



The effect of annealing on InGaAs quantum dots morphology and ordering investigated by triple crystal X-ray scattering in grazing incidence

Experiment number:
HS-3487

| | | |
|----------------------|---|--------------------------------------|
| Beamline: | Date of experiment: from: 25.06.2008 to: 01.07.2008 | Date of report: 22.08.2009 |
| Shifts: 15 | Local contact(s): Amarjeet SINGH | <i>Received at ESRF:</i> |

Daniil GRIGORIEV ^{a)} *

Markus RIOTTE ^{a)} *

Andrey MINKEVICH ^{a)}

Edwin Fohtung ^{a)}

a) Institute for Synchrotron radiation, Forschungszentrum Karlsruhe, 76344 Eggenstein Leopoldshafen, Germany

Martin SCHMIDBAUER ^{b)}*

b) Leibniz-Institut für Kristallzüchtung, Max-Born-Straße 2, D-12489 Berlin, Germany

Report:

Lateral ordering and Morphology evolution of InGaAs (001) QDs due to high temperature post growth annealing

M. Riotte¹⁾, D. Grigoriev¹⁾, E. Fohtung¹⁾, A Minkevich¹⁾, D. Z. Hu³⁾, D. M. Schaadt³⁾ T. Slobodskyy¹⁾, M.Schmidbauer²⁾, and T. Baumbach¹⁾

¹⁾ Institute for Synchrotron radiation, Forschungszentrum Karlsruhe, 76344 Eggenstein-Leopoldshafen, Germany

²⁾ Institute for Crystal Growth. Max-Born-Str. 2 12489 Berlin, Germany.

³⁾ Institute for Applied Physics, UNI-Karlsruhe Kaiserstr 12, 76131 Karlsruhe, Germany.

Introduction

The aim of the present work was to understand the role of strain- and surface diffusion- driven mechanisms in self-organization and formation of InGaAs/GaAs QD ensemble. The influence of post growth annealing was directly observed. A corresponding publication: "Lateral ordering and morphology evolution of InGaAs (001) quantum dots (QDs) due to high temperature post growth annealing" is planned to be submitted end of September 2009.

Sample preparation

The samples were prepared in MBE chamber by deposition of 250 nm thick GaAs buffer layer at 570 °C followed by deposition 2.1 ML InAs at 500 °C. The growth rate of GaAs and InAs are 0.44ML/s and 0.068ML/s respectively. The un-annealed sample was rapidly cooled to room temperature. The other sample was kept at the growth temperature for 5 minutes under constant As flux and then rapidly cooled to room temperature.

Measurement method

The GISAXS measurements were performed with synchrotron radiation at a wavelength of $\lambda=1.54988\text{nm}$. The incoming angle was set to $\alpha_i = 0.7 - 0.8$ degree in order to realize grazing incidence conditions. A position sensitive line detector (PSD) oriented perpendicular to the sample surface was used in combination with an SI(111) analyzer to record the Q_z - dependent scattering. The beam size at the sample position was $0,2(v) \times 0.1(h)$ mm. The sample was then rotated 180 degrees in 3-4 degree steps around its surface normal while at each position a detector-scan in the sample plane was performed in order to obtain 3D reciprocal space data.

The 3D scattered intensity data was integrated over two Q_z -intervals with the same width, but situated at different absolute positions. The first integration was done around the area of specular reflection ($\alpha_f = \alpha_i = 0.7$ resp 0.8 degree) shown in b),e) while the second area of integration was chosen around the Yoneda position ($\alpha_f \approx 0.3$ degree) shown in c), f).

Results

Figure 1. shows a single scan of the PSD. The Yoneda level, the specular reflection as well as a Quantum dot side facet truncation rod are visible. For presentation these scans have been integrated along Q_z in order to obtain the 2D in-plane GISAXS maps (figure 2 c-d).

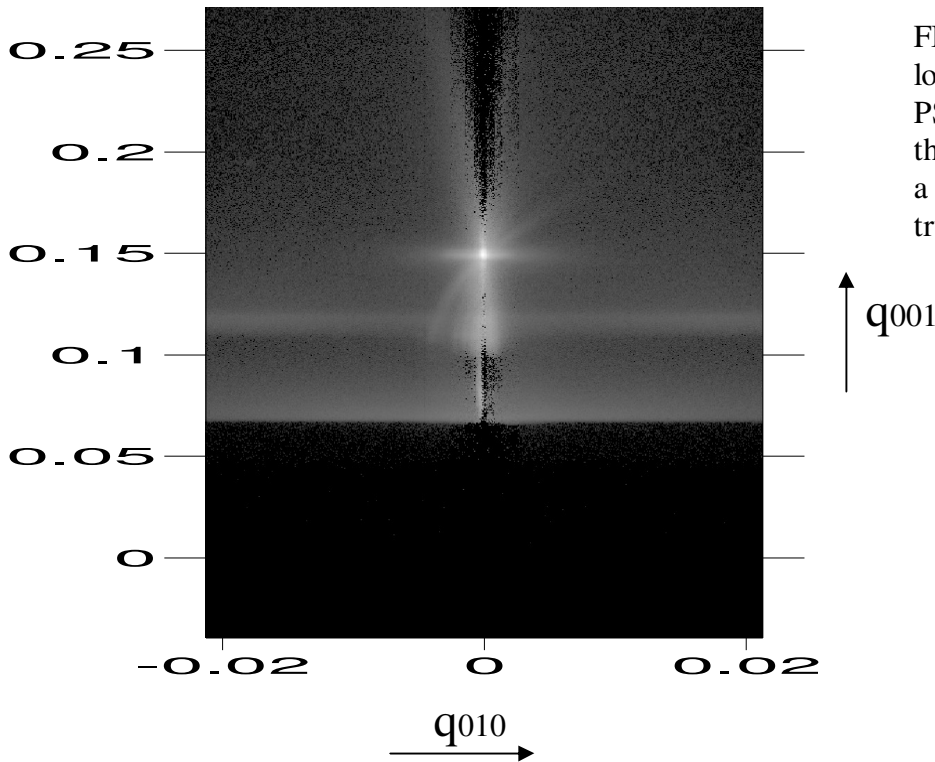


FIG1: Intensity plot in logarithmic scale of a single PSD scan. The Yoneda level, the specular reflection as well as a Quantum dot side facet truncation rod are visible.

In figure 2(a,d) two AFM images of the InGaAs Quantum Dots as grown (left) and post growth annealed for 5 minutes (right) are displayed. The density of the dots decreases from 92 [$1/\mu\text{m}^2$] to 56 [$1/\mu\text{m}^2$] while the average sizes decreases slightly from 56 nm to 48 nm. Concerning the height a decrease from 7.5 to 5 nm is observed. A weak alignment of the Dots in chains can be seen in both cases but more pronounced in the case of the annealed sample.

The in-plane GISAXS reciprocal space maps c) and e) contain the information about side facets and correlation before annealing, while in d) and f) the corresponding information for the sample after annealing.

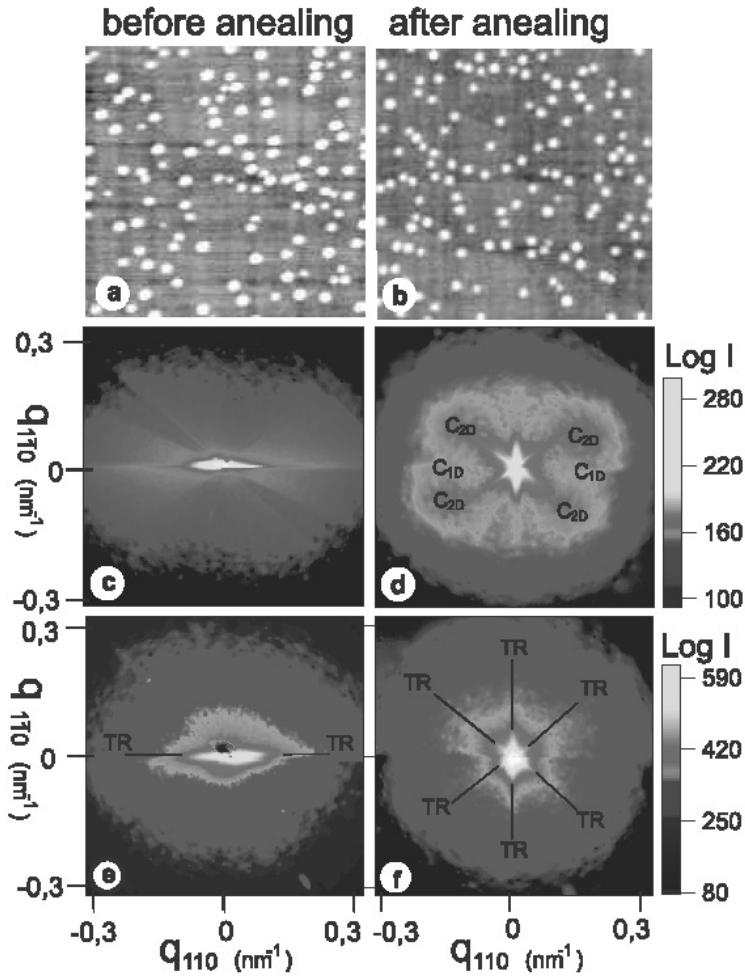


FIG2: Atomic force Micrographs of a 2 x 1 um area showing the QDs before (a) and after annealing (b). The color maps display the in-plane GISAXS data of the non-annealed (c,e) and the annealed sample (d,f). The intensity in reciprocal space was integrated over Q_z around the position of the specular reflected peak in case of image e) and f) and integrated around the Yoneda level in case of c) and d).

In every picture an intense central part corresponds to the truncation rod (TR) cross-section. The intensity streaks coming out of this central part (labeled f) are the QD facet TR projected on the horizontal plane. The full 3D simulation resulted in $\{119\}$ faceted QDs before and $\{117\}$ and $\{017\}$ faceted QDs after annealing. The non-annealed sample (image c) does not show any positional correlation while four correlation peaks P positioned along $\langle 010 \rangle$ are clearly identified for the annealed sample (image f). The distance between opposed peaks is $0,34 \text{ nm}^{-1}$ what corresponds 37 nm in real space and reveals a close neighboring inside the chains visible in the AFM images. All correlation peaks are a little bit deformed towards the two spots C. This could indicate a tendency of alignment in $[0-11]$ chains.

Conclusion:

We observe lateral ordering of the QDs in case of the post growth annealed sample while no ordering can be seen for the non-annealed QDs. We highlight the existence of different correlation types as a result of ordering that occurs to minimize the energy contribution caused by elastic interactions between neighboring dots. A transformation of the dot shape during post growth annealing is reported.